Journal Name

ARTICLE

Synthesis and Physicochemical Characterization of Room Temperature Ionic Liquids and their Application in Sodium Ion Batteries

Received 00th January 20xx,
Accepted 00th January 20xx

DOI: 10.1039/x0xx00000x

www.rsc.org/

Pauline J. Fischer‡[a], Minh Phuong Do‡[b], Robert M. Reich[a], Arun Nagasubramanian[c], Madhavi Srinivasan[b] and Fritz E. Kühn*[a]

Sodium ion batteries (SIBs) based on IL electrolytes have attracted great attention particularly in large-scale energy storage systems for renewable energy due to the abundance of sodium and the high safety resulting from the use of non-flammable ionic liquid (IL) electrolytes. In this article, a series of 15 functionalized room temperature ionic liquids (RTILs) suitable as electrolytes is presented. Special emphasis was laid on purity of the synthesized RTILs and a consistent and uniform characterization of their physicochemical properties. Evaluation of the viscosity, conductivity, thermal and electrochemical stabilities gave rise to clear structure-properties relationships rendering the ether functionalized RTILs most promising for the application in SIBs. Electrochemical investigations of the ether functionalized IL electrolytes in SIB half cells ($Na_{0.6}Mn_{0.9}Co_{0.1}O_2$ as cathode material) proved their compatibility with a SIB system. Stable cycling performance was achieved with the piperidinium based RTIL **IL 6** outperforming the organic electrolyte by far with a retention of 81% after 350 cycles. These results support the suitability of RTILs to enhance the performance of SIB systems and serve as basis for the design of high performance IL electrolytes.

Introduction

Electricity generated from renewable energy sources such as wind, solar or water power offers enormous potential to meet future energy demands.[1] Thus, large-scale energy storage systems have received worldwide attention since they are essential to stabilize the intermittent energy provided by renewable energy sources and help to provide a continuous flow of energy.[2, 3]

Additionally, the growing sector of electrical mobility pushes the development of energy storage systems. Even though lithium ion batteries (LIBs) are the dominant charge storage systems for consumer portable devices, the implementation of Li-based technologies for large-scale energy storage faces significant challenges.[2, 4] Main drawbacks of lithium based systems are limited Li reserves and steadily increasing costs for this alkali metal.[4-6] Using a technology based on sodium as alternative has become a promising focus of research because of its much higher abundance (ratio of reserves Li:Na = 1:1000)[5], lower cost and easy mining of the respective minerals.[3, 7, 8] A further benefit of sodium ion batteries (SIBs) is based on the potential use of low weight and less expensive aluminum current collectors for both electrodes, thus leading to a further reduction of costs.[3, 9] Since Li and Na are neighboring elements in the periodic table, they share similar fundamental principles and properties. Therefore, transfer of the knowledge gained for LIBs over the past two to three decades to SIBs is possible to a certain extent.[8, 10, 11] Nevertheless, the technical performance of SIBs is still far from optimal since sodium based systems have been studied much less than Li based ones, leaving sufficient space for improvements in SIB technology.[7, 11]

In order to implement SIBs in large-scale energy storage systems, safety and long-term cycling of the system are two important challenges.[7, 11] Especially SIB systems with conventionally applied organic electrolytes, e.g. $NaClO_4$ dissolved in a mixture of carbonate based solvents (ethylene carbonate (EC), propylene carbonate (PC), dimethyl carbonate (DMC))[9], pose serious safety issues due to the electrolytes high flammability and volatility and also suffer from poor cycling stability.[7, 12, 13] Among different approaches for safer electrolytes e.g. polymer electrolytes are good candidates, since they do not contain easily flammable, liquid, organic solvents.[14] Different polymer electrolytes have already been successfully tested in various studies.[15-17]

Further, Ionic liquids (ILs) or room temperature ionic liquids (RTILs) are rendered promising alternatives to the highly volatile and flammable organic electrolytes since they exhibit several beneficial properties.[5, 9, 14] ILs are usually considered to be electrochemically and thermally stable. Further, they have an

[a] Molecular Catalysis, Catalysis Research Center and Department of Chemistry, Technische Universität München, Lichtenbergstr. 4, 85747 Garching bei München, Germany.
[b] School of Materials Science and Engineering, Nanyang Technological University, Singapore 639798, Singapore; Energy Research Institute at NTU (ERI@N), Nanyang Technological University, Research Techno Plaza, 50 Nanyang Drive, Singapore 637553, Singapore.
[c] TUMCREATE LTD, #10-03, CREATE Tower, 1 Create Way, Singapore – 530351.
‡ These authors have equally contributed to this work.
* Corresponding author: Prof. Dr. Fritz E. Kühn; E-Mail: fritz.kuehn@ch.tum.de
Electronic Supplementary Information (ESI) available: [details of any supplementary information available should be included here]. See DOI: 10.1039/x0xx00000x

insignificant volatility, and thus a low to negligible flammability.[18-20] The prospect that RTILs can be tailored to meet specific requirements has promoted their application in various fields, e.g. as media for catalysis or chemical synthesis or even as catalysts themselves.[21-25] Especially their high thermal and electrochemical stability combined with a good ionic conductivity render them promising and safe alternatives to the highly flammable conventional organic electrolytes as well.[22, 26] Recent reports show that RTILs are able to enhance the capacity and cycling stability of SIBs underlining their suitability as promising electrolytes.[4, 7, 10, 11, 27] A further advantage of RTILs as electrolytes is the facile tunability of their physicochemical properties by modifying the anion or cation. For instance, variations of the core structures or introduction of functional groups can have significant effects on the physicochemical properties. Up to date, only few RTILs including mainly unfunctionalized imidazolium and pyrrolidinium ILs have been evaluated in SIB systems, though.[3, 5, 9] Taking lithium-based systems into account, a much broader range of RTILs has been investigated as electrolytes.[14, 26, 28] However, the evaluations of the electrochemically relevant IL properties suffer from diverse variations of the conditions and systems in which the RTIL electrolytes were tested. Therefore, direct comparison and meaningful conclusions of the structure-properties relation are hardly possible. In order to obtain comparable data and draw reliable conclusions of the structural impact of different functionalized RTILs on physicochemical properties, a systematic and uniform approach is indispensable. Therefore, in this work a series of novel as well as literature known RTILs with different N-based core structures, functional groups and anions is presented and examined. Focus is laid on the consistent characterization of the RTILs especially with respect to parameters relevant for electrochemical applications like viscosity, conductivity as well as thermal and electrochemical stability. Based on these characteristics, the most promising RTILs were applied as electrolytes in a SIB half-cell with $Na_{0.6}Mn_{0.9}Co_{0.1}O_2$ (NMO) as cathode material. This Co-doped NMO material was recently reported to exhibit enhanced performance compared to previously applied undoped sodium-manganese-oxides.[13] Evaluation of the electrochemical performance of the selected ILs gives rise to a deeper understanding of the structure-performance relationship. This knowledge can pave the way to tailored RTIL electrolyte combinations suitable for stable and safe SIBs in the future and will help to conquer the energy challenges of the 21st century.

Results and discussion

Selection of suitable RTILs as electrolytes

The selection of the cationic core structures for the evaluated RTILs was based on the respective electrochemical stabilities. For their application in battery systems, a wide electrochemical stability window (ESW) of the ILs is of great importance to prevent electrochemical decomposition of the electrolyte. Imidazolium based ILs are known for their inferior reductive as well as oxidative stability and were therefore not considered in this study.[26, 28] In contrast, piperidinium, pyrrolidinium and tetraalkylammonium based ILs have been shown to exhibit outstanding electrochemical stabilities up to 6 V, rendering them as suitable core structures for IL electrolytes.[26, 28, 29]

In order to reduce the viscosity and enhance the conductivity of the RTILs, asymmetric core structures like NEt_2Me on the one hand, or ether substituents on the other hand, have been proven to be advantageous.[28-31] When incorporating ether- or other functional groups, the length of the NC-spacer between the quaternary nitrogen and the carbon attached to the functional group has a significant influence on the thermal stability of the cation. It was shown that cations with a methyl linker exhibit considerably lower thermal stabilities than their analogues with an ethyl- or longer linker.[32] Therefore, all functional groups in this study were tethered to the respective nitrogen atom via an ethyl-linker in order to achieve high thermal stabilities.

Another important characteristic of an electrolyte is its solid electrolyte interface (SEI) layer formation ability. To achieve good cycling stability the formation of a stable SEI layer on both electrodes, preventing further electrolyte decomposition, is essential.[14, 28] Nitrile, allyl and ester groups are known to improve cell performance by supporting the formation of a stable SEI layer and were thus included in the present study.[28, 33-36] Additionally, ester substituents are able to improve the solubility of conducting slats when compared to unfunctionalized analogues.[37]

Regarding the anion, focus was set on the two imide anions bis(trifluoromethane)sulfonimide (TFSI) and bis(fluorosulfonyl)imide (FSI) since they are known to form room RTILs and account for comparably low viscosities. FSI ILs tend to exhibit even lower viscosities and higher conductivities compared to TFSI ILs and are said to have superior SEI layer forming abilities.[30, 31] TFSI ILs on the other hand show higher thermal and electrochemical stabilities and are less cost-intensive.[26, 28]

Synthesis of various RTILs

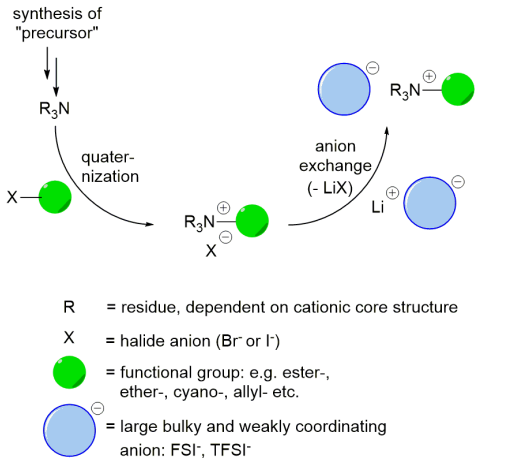

Figure 1: Schematic procedure of the synthetic route applied in the RTIL syntehsis.

All RTILs were synthesized under similar conditions according to a two-step reaction protocol starting from the respective tertiary amine (Figure 1) in 47 to 90% yield. In order to introduce the desired functional group, the tertiary amine was reacted with the respective alkyl halide in a nucleophilic substitution reaction. Subsequent exchange of the rather hard and strongly coordinating halide anion with a large and bulky, weakly coordinating anion, like TFSI and FSI, converts the quaternary ammonium salt to the respective RTIL. All synthesized RTILs were thoroughly purified in several washing steps followed by additional purification using activated charcoal. A water content below 5 ppm was ensured by drying the pre-dried ILs at 70 °C under ultra-high vacuum (10^{-6} mbar) for at least 24 h. The RTILs synthesized for this study are shown in Figure 2 (newly synthesized ILs are depicted in blue) and their respective physicochemical properties are listed in Table 1. For the sake of convenience, the ILs were abbreviated by numbers as indicated in Figure 2. Further, Pyr, Pip, Mor and N_{222}/N_{221} (1 = methyl, 2 = ethyl) denote the applied cationic core structures: pyrrolidinium, piperidinium, morpholinium and ammonium. Full characterization was carried out via ^{1}H and ^{13}C NMR spectroscopy, electrospray ionization mass spectrometry (ESI MS) and elemental analysis. The characterization data is fully consistent with the expected compositions and structures and documents the high purity of each compound.

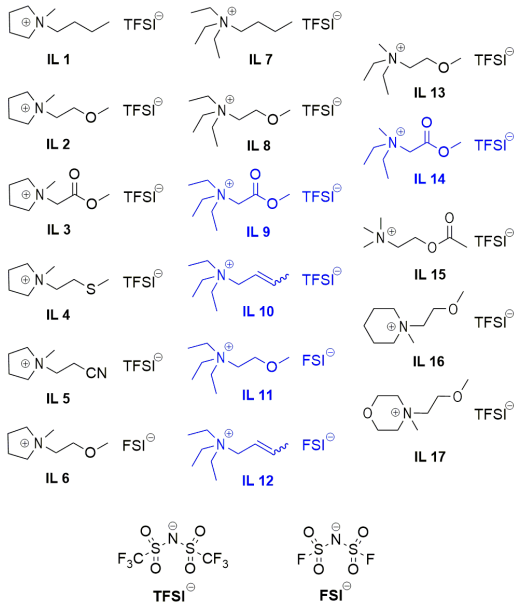

Figure 2: Overview of the RTILs synthesized in this study (novel ILs depicted in blue). **IL 1** & **7** were not synthesized but obtained from commercial sources and purified.

Applied methods of characterization

The increasing amount of literature published on ionic liquids generates an extensive quantity of data including manifold information regarding the properties of RTILs.[38] This data serves as basis for further investigations, however it has to be handled with great care. Most characterization techniques are highly dependent on the method and setup applied as well as the evaluation procedure making a direct comparison between different sets of data very vague and not always reliable. A further major drawback of the reported data is the number of studies performed with impure or wet ILs making some results dubious and somewhat hindering the development in this field.[9] Therefore, exceptional emphasis was put on the purity of RTILs and their uniform and consistent characterization in this study. For the application of RTILs as electrolytes, viscosity, conductivity and thermal as well as electrochemical stability are crucial parameters and were thus evaluated for the RTILs presented herein.

Viscosities: The comparably high viscosities of RTILs is one of the largest barriers for their application as pure electrolytes.[29] Both ion diffusion and conductivity in an electrolyte, and consequently the capacity of a battery cell, is highly dependent on the electrolytes viscosity. Therefore, the fundamental understanding of the factors, which influence the viscosity of RTILs, is of essential importance for the design and choice of suitable RTIL electrolytes.[29] The dynamic viscosity η is a physicochemical property, which is largely governed by species interactions such as van der Waals interactions, hydrogen bonding, and columbic forces. Further, flexibility and conformational freedom as well as the molecular mass and the shape of the respective ILs have been found to affect the viscosity.[29, 39, 40] It has to be noted that viscosity values can fairly vary depending on the measuring technique and setup. Considering this, all RTILs evaluated in this study where surveyed under identical conditions with one rheometer to enable a valid comparison (Table 1).

When comparing TFSI ILs containing the same cationic core structure, clear trends regarding the functional groups can be observed. The lowest viscosity was detected for the ether functionalized pyrrolidinium **IL 2** (63 cP). Compared to the unfunctionalized analogue **IL 1** (84 cP), the lower viscosity of the ether functionalized IL can be attributed to the increase of conformational degrees of freedom due to the higher flexibility of the ether side chain. This effect seems to outperform the stronger polar interactions resulting from the substitution of a C atom by the more electronegative O atom.[29, 30, 41] The same trend can be observed for the ammonium based TFSI ILs: **IL 8** (98 cP) and **IL 13** (80 cP). Both exhibit lower viscosities than **IL 7** (156 cP). When moving to sulfur as the higher homologue of oxygen, the impact of the stronger van der Waals interactions contributes to the enhanced viscosity of **IL 4** (222 cP) compared to **IL 2** (63 cP) and **IL 1** (84 cP). The viscosity is also increased considerably upon introduction of an ester functionality into the side chain:

IL 3 (287 cP) > **IL 1** (84 cP) > **IL 2** (63 cP)

IL 9 (312 cP) > **IL 7** (156 cP) > **IL 8** (98 cP)

IL 14 (292 cP) > **IL 13** (80 cP).

Stronger dipole-dipole interactions in combination with additional hydrogen bonding account for the enhanced viscosity in these cases.[42] For the same reason, the viscosity of **IL 5** (534 cP) is comparably high.

In contrast to the side chain functionalization, an ether group incorporated in the cationic core results in a strong increase of viscosity. This effect is illustrated when comparing the two ILs containing a 6-membered ring: **IL 16** (123 cP) and **IL 17** (376 cP).

Introduction of the ether bond in the 6-ring does not lead to an enhancement of the conformational degrees of freedom due to the rigid structure of the 6-ring. Rather, the strong polarization induced by introduction of O determines the molecular interactions and therefore the viscosity.[29]

When comparing the viscosity of all ether as well as ester-functionalized TFSI ILs, the following trend for the dependency of the viscosity on the cationic core structure can be found (from the lowest to the highest viscosity): Pyr < N_{221} < N_{222} < Pip < Mor. Excluding the functionalized core structure of the morpholinium IL, these trends can be explained taking the impact of the ion shape into account. The decrease in viscosity for the ammonium ILs **IL 8** (98 cP) / **IL 9** (312 cP) vs. **IL 13** (80 cP) / **IL 14** (292 cP) respectively, is caused by the asymmetry and smaller size of the N_{221} cation.[39, 40, 42] Furthermore, for the ring structured ILs, the piperidinium core most likely accounts for a higher viscosity due to its chair conformation and high rigidity. On the other hand the relatively low viscosity of the pyrrolidinium ILs (e.g. compared to an acyclic ammonium cation with an identical number of carbon atoms) seems to result from the quasi-flat geometry of the pyrrolidinium cation preventing any increases due to steric effects or entanglement.[43]

The TFSI anion as well as the FSI anion are characterized by improved charge distribution and higher flexibility compared to other commonly applied anions, like BF_4^- or PF_6^- and therefore account for comparably low viscosities.[43] For ILs with the same cation, FSI based ILs exhibit lower viscosities than their TFSI analogues, as evident from:

IL 6 (44 cP) < **IL 2** (63 cP)

IL 11 (72 cP) < **IL 8** (98 cP)

IL 12 (120 cP) < **IL 10** (156 cP).

This is expected, as the van der Waals interactions are decreased for the smaller FSI-anion compared to TFSI.[30, 41]

Conductivities: The conductivity of an electrolyte is mainly governed by its viscosity, molecular weight and ion size.[44] The higher the viscosity of the electrolyte and the larger and bulkier its components, the harder it is for ions to move past each other resulting in lower conductivities. Figure 3 exemplarily shows the comparison of viscosity and conductivity for the pyrrolidinium based TFSI RTILs. The respective Walden plot is given in Figure SI 2. A decreasing conductivity for the ILs with increasing viscosity can be detected confirming the inversed connection between these two properties.

Conductivities of around 1 mS/cm for the RTILs with high viscosities (> 280 cP) up to 7.66 mS/cm for the least viscous IL (**IL 6**, 44 cP) were obtained.

Table 1: Physicochemical properties of the characterized RTILs. [a] Viscosities and conductivities determined at 23 °C. [b] Electrochemical stabilities vs. Fc/Fc^+.

IL number	η [cP][a]	σ [mS/cm][a]	T_d [°C]	E_A [V][b]	E_C [V][b]	ESW [V]
1	83.5	3.26	427.5	2.49	-2.65	5.14
2	63.0	5.26	408.6	2.35	-2.63	4.98
3	287.1	1.27	351.9	2.55	-2.49	5.04
4	222.4	1.68	286.0	1.19	-2.76	3.95
5	533.8	1.28	163.4	2.71	-2.20	4.91
6	43.6	7.66	271.2	2.22	-2.67	4.89
7	156.0	1.94	396.2	2.55	-2.75	5.3
8	98.2	2.92	390.3	2.39	-2.69	5.08
9	312.2	1.02	410.8	2.57	-2.46	5.03
10	156.2	1.91	345.9	2.18	-2.69	4.96
11	71.8	5.07	280.4	2.29	-2.73	5.02
12	119.7	3.81	261.2	2.08	-2.74	4.82
13	80.1	3.99	406.5	2.34	-2.58	4.92
14	291.5	1.20	346.1	2.55	-2.41	4.96
15	256.5	1.76	367.7	2.54	-2.63	5.17
16	123.4	2.64	403.7	2.32	-2.64	4.96
17	375.8	1.01	395.1	2.29	-2.67	4.96

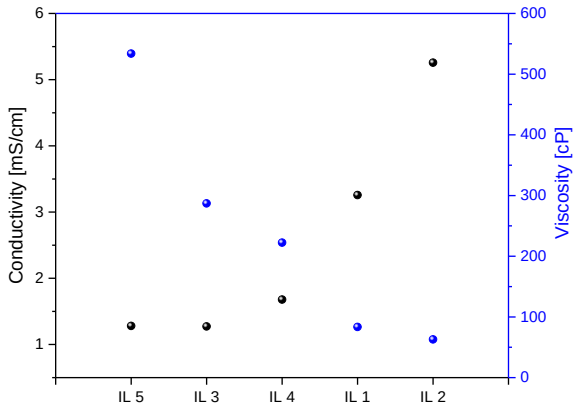

Figure 3: Correlation of conductivity and viscosity for the functionalized pyrrolidinium TFSI ILs.

Thereby, especially the less viscous ILs exhibit conductivities which are more than sufficient for electrochemical applications.[45] In agreement with the viscosities, especially the introduction of an ether group in the IL side chain and the replacement of the TFSI anion by FSI enhance the conductivity of the respective ILs. On the other hand, comparing **IL 5**, **IL 17** and **IL 9** the conductivity values do not strictly follow the viscosity trend. This implies that besides viscosity, nature and spatial structure of the IL cation have an impact on the conductivity as well. It is worth noting that the difference in conductivity values becomes significantly smaller with increasing viscosity. When comparing the ester functionalized TFSI ILs (**IL 3, 9, 14, 15**), which all exhibit relatively high viscosities (257 – 312 cP), only a very small difference in their conductivities is noticeable (1.0 – 1.8 mS/cm). Same applies for **IL 3** and **IL 5**, which show high viscosities (>280 cP) and nearly equal conductivities (~1.28 mS/cm). In contrast, a strong impact of the viscosity on the resulting conductivities (2.6 – 7.7 mS/cm) can be observed for the low viscous ether functionalized ILs (**IL 2, 6, 8, 11, 13, 16**). This phenomenon has been reported before and suggests that the transport of ions in highly viscous salts is less dependent on the viscosity.[29] As expected, conductivities increase significantly with rising temperatures - about one order of magnitude between 20 and 80 °C - due to the decrease of viscosity and the enhanced ion movement at higher temperatures (Figure SI3).[8, 30, 45, 46] Furthermore, it is well known that in contrast to aqueous media, the conductivities of ILs decrease upon addition of a conducting salt.[41, 46, 47] Such behavior is most likely caused by strong electrostatic interactions of the ions of the conducting salt with the ions of the IL resulting in an increased viscosity of the mixture. As stated in literature[11, 48] a non-linear decrease of conductivity with increasing NaFSI concentration was observed for **IL 1** exemplarily (Figure SI4). Further, Figure SI5 shows the decrease of conductivity upon addition of the conducting salt NaFSI (0.5 M) for selected ILs, clearly underlining this phenomenon. In accordance to literature, the addition of the conducting salt to ester functionalized ILs results in less decrease in conductivity compared to alkyl or ether functionalized ILs underlining the enhanced salt dissolving properties of ester functionalized ILs.[46]

Thermal stability: Non-flammability and high thermal stability are key factors, which render ILs as superior electrolytes in terms of safety especially compared to the conventionally applied highly flammable organic electrolytes.[14, 27, 45] Thermal stability of the RTILs **1 – 17** was investigated by thermogravimetric analysis (TGA) and is defined by the decomposition temperature T_d. Since literature provides several different evaluation techniques to define the thermal stability from a TGA curve, an exact and uniform evaluation is barely possible. The common methods used to determine thermal stability include e.g. a certain percentage of mass loss, the decomposition temperature T_d or the onset temperature T_{onset}. The contributions of the measurement process to the obtained results should not be underestimated as well: e.g. only the variation of the heating rate has been shown to influence the obtained results.[38] Additionally, it shall be noted that two different stability types and measuring techniques have to be distinguished. The usually reported short-term thermal stability, which is also considered in this study, is accessible via ramped TGA. In contrast, several publications deal with the long-term thermal stability (accessible via isothermal TGA) and can therefore not be taken into consideration for comparison.[49] All investigated TFSI RTILs (with exception of **IL 5**) display high thermal stabilities with decomposition temperatures ranging from 346 °C to 428 °C (Table 1) and are therefore suitable electrolytes for safe battery systems. Figure SI6A clearly shows that the nature of the anion has a strong impact on the thermal stability. Consistent with literature, the FSI based **ILs 6**, **11**, **12** exhibit significantly lower T_d-values than their TFSI analogues **IL 2**, **8**, **10** (Δ_{max} = 138 °C) regardless of the cationic species.[38, 41, 50] Most likely, the higher liability of the FSO_2-group in the FSI anion towards pyrolysis accounts for this behavior.[41, 50]

Thermal decomposition of the cation generally proceeds via the reverse *Menshutkin reaction* (dealkylation). Thus, usually loss of the alkyl chain leads to decomposition regardless of the cationic core structure.[32, 38] This is in accordance with the observation that for ILs with different core structures but same anion and functional group, only small differences in the T_d are apparent. Figure SI6B confirms this trend for the ether functionalized TFSI **ILs 2**, **8**, **13**, **16** and **17** where only the core structure is varied. Therefore, the cationic core structure has less impact on thermal stabilities than the anion.

Among all evaluated RTILs, the unfunctionalized **IL 1** exhibits the highest thermal stability with a T_d of 428 °C. As reported in literature, the thermal stability is slightly reduced with the introduction of an ether function in **IL 2** to 409 °C. The synergistic electron-withdrawing effect of the N and O atoms render the alkyl chain more susceptible towards nucleophilic attack and therefore make it easier to cleave.[32, 45, 51] Same behavior is observed for the ammonium salts **IL 7** (396 °C) and **IL 8** (390 °C).

Comparison of all analyzed Pyr TFSI ILs (**IL 1 – 5**) (Figure SI6C) reveals further trends caused by the respective functional groups. As mentioned before, the unfunctionalized

pyrrolidinium **IL 1** shows the highest stability followed by the functionalized **IL 2** (409 °C), **IL 3** (352°C) and **IL 4** (271 °C). The lowest thermal stability was detected for **IL 5** (163 °C). Its decomposition takes place in two steps suggesting the loss of the nitrile group in the first and dealkylation in the second step.

Electrochemical stability: Since electrolytes for electrochemical applications should be preferably resistant towards oxidation and reduction, it is of great importance to evaluate the electrochemical stability windows (ESWs) of potential electrolytes in advance to their application.[26] The latter is defined as the range between the cathodic (E_C) and the anodic (E_A) stability limits in which the involved anions and cations are not reduced or oxidized.[49] Stability limits of numerous ILs have already been reported in literature, however comparison of the data is difficult as the measurement conditions have a significant impact on the reported ESWs of the ILs.[49] Most importantly, the voltammetry curves are recorded using different working electrodes (e.g. glassy carbon, Pt, Au, W) and against various references (e.g. Ag/Ag^+, Li/Li^+, I^{3-}/I^-, Fc/Fc^+ (Fc = ferrocene)). All these parameters have different effects on the electrochemistry of the evaluated ILs.[26, 28] The measurement set up, especially the volume of the measuring cell and the distance of the electrodes, have a significant influence on the results as well. Further, the conditions (mostly a defined current density) under which the stability limit of the electrolyte is reached, is not clearly defined. This makes the exact determination of the ESW somewhat arbitrary.[52]

The herein reported ESWs were detected by linear sweep voltammetry (LSV) in a three-electrode setup using a glassy carbon working electrode and a Pt wire as counter electrode. All values were referenced to the Fc/Fc^+ redox couple. The respective cathodic and anodic stability limits were defined as the potentials at the cut-off current density of 1 mA/cm^2 in the first scan.[49] The unfunctionalized TFSI ILs **IL 1** and **IL 7** exhibit very wide ESWs of 5.14 V and 5.3 V, respectively. However, most of the functionalized ILs in this study show only slightly lower ESWs of around 5 V (4.82 V – 5. 17 V) and are therefore suitable for high voltage applications as well.[40] The functionalized RTILs are thought to outperform the unfunctionalized ILs in terms of conductivity, SEI layer formation and overall cell performance. Therefore, their in some cases slightly lower electrochemical stability is rendered less important. Only the thioether functionalized **IL 4** exhibits a narrow ESW of 3.95 V due to the high susceptibility of the thioether towards oxidation and is thus not considered as stable enough.[49, 53]

In order to understand the respective overall stability ranges, the accurate stabilities towards reduction (E_c) and oxidation (E_A) are crucial. According to literature, the E_c is mainly affected by the nature of the cation and the E_A by the nature of the anion.[28, 41, 49, 51, 54] Within this study, we focused on the susceptibility of the ESW to three major factors: anion, cationic core structure and functional group of the respective ILs.

When comparing the LSVs of the pyrrolidinium based TFSI ILs (**IL 1 – 5**) depicted in Figure 4A, a clear influence of the functional groups on the cathodic stability limit can be observed. Whereas **IL 2** (-2.63 V) and **IL 4** (-2.76 V) show cathodic stabilities close to the unfunctionalized **IL 1** (-2.65 V), **IL 5** (-2.20 V) and **IL 3** (-2.49 V) exhibit fairly higher E_C values. The inferior cathodic stability of the latter two compounds is most likely caused by facile reduction of the ester or nitrile group, respectively. Decent cathodic stabilities for the ether functionalized (around -2.64 V) and higher E_C values for the ester functionalized (around -2.44 V) ILs can be observed for the ammonium based TFSI ILs (**IL 8**, **9**, **13**, **14**) as well (Figure 4B). A slight dependence of the E_C on the cationic core structure is apparent when comparing ILs with a N_{222} core (**IL 8**, **9**) to their analogues with a N_{221} core (**IL 13**, **14**). A difference of 0.05 V for the ester and 0.11 V for the ether functionalized ones was detected. Comparison of the ether functionalized TFSI ILs without functionalized core structure (**IL 2**, **8**, **13**, **16**) in Figure 4B and Table 1 shows differences of about 0.1 V for the cationic core structures. This small shift in the reduction potentials is most likely due to a slight variability in the shielding of the respective nitrogen atoms as previously reported for the ammonium core structures.[55] The effect of the cationic core structure is even less pronounced for the anodic stability. As shown in Figure 4B for the ether functionalized TFSI ILs (**IL 2**, **8**, **13**, **16**) and the ester functionalized TFSI ILs (**IL 3**, **9**, **14**), almost no difference in the anodic stabilities can be observed for different cationic core structures but same functional groups

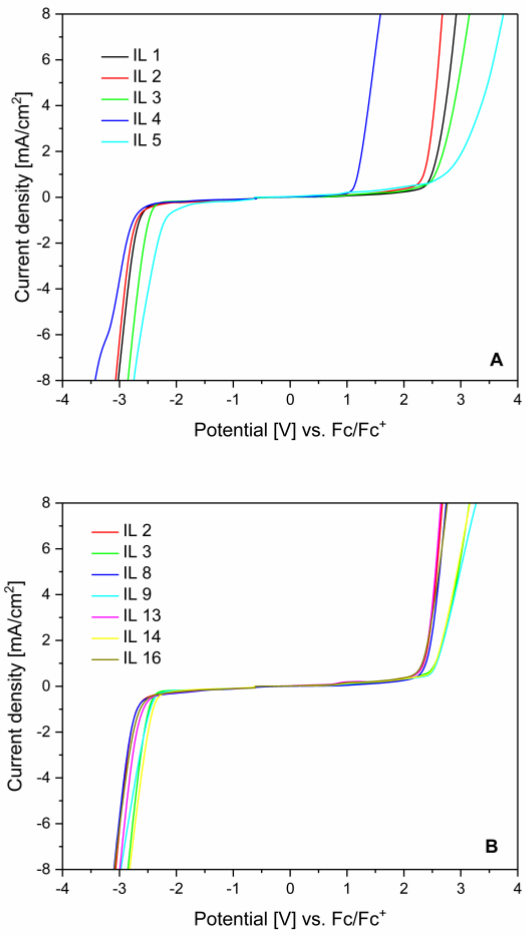

Figure 4: Linear sweep voltammograms of the pyrrolidinium based RTILs (**A**) and the ether vs. ester functionalized RTILs (**B**).

(ether or ester). The E_A values also differ far less than 0.1 V. These results imply that the cationic core structure has a small effect on the cathodic stability and a negligible effect on the anodic stability. In contrast, the anodic stability is influenced significantly by functional groups independent of the cationic core structure to which they are attached. As shown in Figure 4A, a broad anodic stability range reaching from 1.19 V for **IL 4** to 2.71 V for **IL 5** can be covered. As mentioned before, the low oxidative stability of the thioether substituted **IL 4** is most likely caused by the high susceptibility of the thioether towards oxidation thus being oxidized prior to the TFSI anion.[49, 53] All other cations should be more stable than the respective FSI or TFSI anion in the investigated ILs. Therefore, E_A of these ILs shall depend on the oxidation potential of the anions and not differ with the cation at first sight. However, based on the herein reported data, an influence of the cation on the anodic stability is evident. Such an impact has been reported before and is associated to a certain type of interaction and de/stabilization between the interacting ions.[26, 49, 51, 56] More investigations to clarify this observation are necessary and will be undertaken in the future. It shall be noted that the anodic stability is further slightly influenced by the choice of the anion of the respective IL. In accordance to literature, the evaluated FSI ILs **IL 6** (2.22 V), **IL 8** (2.29 V) and **IL 12** (2.08 V) show inferior anodic stability compared to their respective TFSI analogues **IL 2** (2.35 V), **IL 8** (2.39 V) and **IL 10** (2.18 V) due to the better resistance of the TFSI anion towards oxidation.[41]

In general, the reported E_c as well as E_A values indicate that the electrochemical stability limits are mainly influenced by the functional group incorporated in the IL cation and less by the anion or the cationic core structures. As shown in Figure SI8 and Table SI2 for selected ILs, addition of NaFSI as conducting salt (0.5 M) has a beneficial effect on the ESW. Such an increase of the ESW by the addition of salt is well known for aqueous so called "water-in-salt" electrolytes.[57-59]

Evaluation of RTIL properties

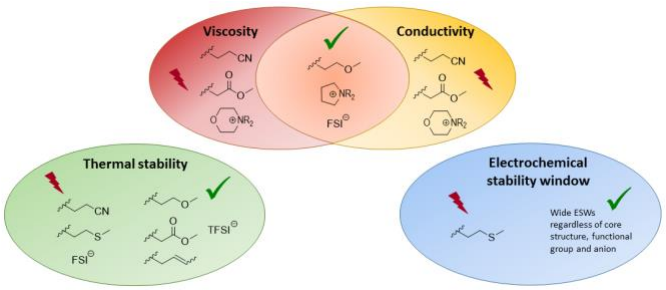

Figure 5: Schematic summary of the main trends observed for the investigated physicochemical properties.

The main trends of the discussed physicochemical properties are summarized in Figure 5.

Viscosity and conductivity are in close relation and are mainly affected by the functional groups tethered to the different cationic core structures. Ester-substituents enhance viscosity and therefore lower conductivity for all core structures, while ether groups have exactly opposite influence. The nitrile group is responsible for the highest viscosity reported in this work. Allylic as well as thioether functionalization result in intermediate viscosities and conductivities. The morpholinium cation is the only core structure with a significantly disadvantageous effect on viscosity and conductivity. Lowest viscosities and vice versa highest conductivities were detected for ILs with pyrrolidinium core and FSI anion.

Thermal stability is lowered significantly for all RTILs containing the FSI anion regardless of the cation. Further, incorporation of a nitrile or thioether group results in thermally less stable ILs. The cationic core structure was found to have negligible influence on thermal stability.

Besides the electrochemically unstable thioether functionalized **IL 4**, all synthesized RTILs show high ESWs which mainly differ in their distinct anodic (E_A) and cathodic (E_C) stability limits.

To gain insights into the electrochemical performance of the ILs in SIBs and their compatibility with the electrode materials, authentic cell tests in coin cells have to be performed. Therefore, a preselection of the most promising RTILs based on the evaluated physicochemical properties was made. From the above observations however, it is obvious that compromises regarding the optimal physicochemical properties have to be made when it comes to such a selection. Combination of all features beneficial for an electrolyte, i.e. good viscosity/conductivity, high thermal stability and good SEI layer formation abilities, in one single IL is hard to achieve. Just to name two examples: the least viscous RTIL with the highest conductivity, **IL 6**, suffers from reduced thermal stability. Further, nitrile functionalization is said to enhance SEI layer formation ability of electrolytes.[28, 33] Contrarily, the nitrile group also accounts for very high viscosity reducing the applicability of **IL 5** as pure electrolyte. The drawbacks of the sole ILs might be overcome by combinations of ILs with different properties. However, to attain a meaningful approach, the electrochemical performance of the pure ILs has to be evaluated first. Once having the performances of different RTILs in hand, a reasonable selection for suitable combinations can be made.

Due to their superior viscosity/conductivity properties, ether functionalized ILs are ideal starting materials for first electrochemical investigations in coin cells. Moreover, the thermally more stable TFSI based ILs were preferred over FSI based ones, since enhanced safety is a main goal in future SIB technology. Different Na^+-transport and SEI layer formation properties are expected when varying the cationic core structure. Taking all these considerations into account, evaluation of the electrochemical performance of the pyrrolidinium, piperidinium and ammonium ether-functionalized ILs **IL 2**, **8**, **13** and **16** in SIB half cells was rendered most meaningful to start with. Electrolytes consisting of the selected ILs with NaFSI (0.5 M) as conducting salt were thus prepared and applied in the coin cell studies explained in the following.

Electrochemical performance in SIB half cells

Galvanostatic cycling: The electrochemical performance of the selected IL based electrolytes and their compatibility with the active materials was tested by galvanostatic cycling in NMO half cells. The coin cells **CC_2**, **CC_8**, **CC_{13}** and **CC_{16}** with the respective electrolytes containing **IL 2**, **8**, **13** and **16** were first charged to 3.8 V, followed by discharging to 1.5 V at a rate of 50 mA/g. For comparison a NMO half-cell with the conventionally employed organic electrolyte EC/PC (1/1 wt%) with $NaClO_4$ (1 M) (**CC_{Org}**) was cycled under same conditions. Cycling data for the first 350 cycles is depicted in Figure 6A. Table 2 shows the initial discharge capacities, retention values and respective diffusion coefficients. Following observations can be summarized concerning the cycling behavior (Table 2):

(i) The cells with IL based electrolytes (**CC_2**, **CC_8**, **CC_{13}**, **CC_{16}**) show inferior initial discharge capacities (100 – 169 mAh/g) compared to **CC_{Org}** (176 mAh/g), while **CC_2** displays the best initial capacity (169 mAh/g) of all IL electrolytes tested.

(ii) Three (**CC_8**, **CC_{13}**, **CC_{16}**) of the four cells with IL electrolytes show significantly better capacity retention (69 - 81%) than **CC_{Org}** (32%) after 350 cycles.

(iii) **CC_{16}** shows the highest capacity retention with 81% of the initial capacity being retained after 350 cycles.

(iv) **CC_2** exhibits the worst performance – even lower than **CC_{Org}** – in spite of the high initial capacity.

Further, the charge-discharge curves of the respective cells are given in Figures SI9 and SI10 and show that the fading in cycling performance correlates well with voltage fading. **CC_{Org}** and **CC_2**, which display the worst retention also have the highest polarization occurring with cycling, while **CC_{16}**, which has the highest retention, displays the lowest voltage fading.

Viscosity and conductivity of an electrolyte influence its ion transport properties and thus can have an impact on the initial capacity of the evaluated cell. Therefore, the higher viscosities and lower conductivities of ILs (Table 1) most likely account for the lower initial capacities of the cells with IL electrolytes compared to **CC_{Org}**. Within the cells with IL electrolytes (**CC_2**, **CC_8**, **CC_{13}**, **CC_{16}**), the trend of the initial capacities can be correlated to the trends of the viscosity/conductivity of the respective ILs. Poor cycling stability for NMO half cells with the organic electrolyte has been reported before and was mainly attributed to phase transitions in the cathode material during the charge – discharge processes.[13] However, the superior performance of the cells with IL electrolytes **CC_8**, **CC_{13}**, **CC_{16}** over **CC_{Org}** can be a result of multiple synergistic effects. Firstly, it is known that the formation of a stable SEI layer during the first cycles is crucial for cell durability. In contrast to organic electrolytes, IL based electrolytes have been shown to result in the formation of a more stable/conductive SEI layer in SIBs. Such a layer prevents continuous electrolyte decomposition thus enhancing cycling stability.[27] Similarly, the dissolution of Mn^{3+} is a common reason for capacity fading of cells with organic electrolytes and might also be reduced when employing IL electrolytes.[10] Further, capacity losses arising due to phase transition of the active material during the charge – discharge processes might be less pronounced when employing certain IL electrolytes.

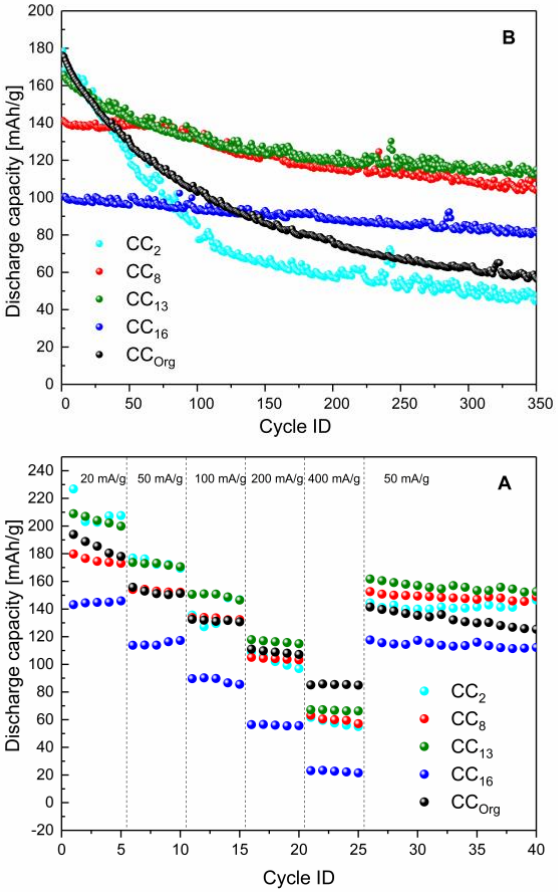

Figure 6: Electrochemical data for the performed SIB half-cell studies. Long term cycling performance until 80% retention of the best cell **CC_{16}** (**A**) and rate test (**B**).

Since the instability of **CC_{ORG}** could also result from the perchlorate anion, the effect of the conducting salt on the cycling stability of NMO half-cells was studied. Therefore half-cells containing EC/PC and different conducting salts ($NaClO_4$, NaFSI and NaTFSI, Figure SI11) were subjected to galvanostatic cycling. No major difference could be observed in cycling stability suggesting, that the organic solvent mixture has a greater effect on stability than the conducting salt in case of the evaluated system.

The exact reasons for the respective cycling stabilities – i.e. the superior performance of **CC_8**, **CC_{13}**, **CC_{16}** and the poor performance of **CC_2** and **CC_{Org}** – require detailed studies of the electrode materials and the nature of the surface layers formed on them. However, the observations made herein hint towards a beneficial effect of piperidinium-based electrolytes on cell stability. Whereas, the pyrrolidinium core seems to be less compatible with the SIB system.

Rate testing: To evaluate the performance under conditions of fast charge and discharge, rate tests with rates ranging from 20 to 400 mA/g were performed. Taking the results from the rate test (Figure 6B) into account, following observations can be made:

(i) At the highest rate (400 mA/g), CC_{Org} shows the highest discharge capacity (86 mAh/g).
(ii) Among the cells with IL based electrolytes, CC_{13} has the best rate performance (68 mAh/g at 400 mA/g), followed by CC_8 and CC_2 while CC_{16} shows lowest capacity. This is in accordance to the cycling behaviour described above.
(iii) CC_8, CC_{13} and CC_{16} are stable to high rate cycling as revealed by retention of capacity at 50 mA/g after high rate cycling. This result indicates that these systems are reasonably stable to reversible sodiation at high rates and no considerable side reactions occur during cycling.[1]
(iv) CC_2 and CC_{Org} are clearly affected by fading and are unable to retain their capacity at 50 mA/g after high rate cycling indicating an instability of these systems to high rate cycling.
Enhanced high rate performance of cells with the organic electrolytes compared to cells with IL electrolytes has been reported before and is mainly due to the relatively high viscosity and low conductivity of the IL electrolytes.[4] For further explanation of the rate test results, apparent sodium-ion diffusion coefficients were determined using cyclic voltammetry and provided in Table 2. It has to be noted that the given sodium-ion diffusion coefficients are only rough estimations and not "physical quantities", since the conditions for applicability of Randle-Sevcik equation are not strictly met. Among the IL electrolytes, the corresponding sodium diffusion coefficients show the highest values for **IL 13** in CC_{13} and the lowest for **IL 16** in CC_{16}. The higher the viscosity of the electrolyte the lower the ion mobility resulting in a low diffusion coefficient and reduced capacity. Generally, the trend obtained in diffusion coefficient studies is consistent with the high rate test performance. At higher rates, the combined effect of Na^+ ion transport coupled with the reduced kinetics of intercalation result in lower capacities for the cells containing IL electrolytes compared to the organic electrolyte. While, from a fast charge perspective, the numbers still have room for improvement, it should be noted that there is scope for further optimization of the electrolyte (i.e. modification of its viscosity/conductivity via additives or mixtures) and thus improving capacity at higher rates. Overall, the results are very promising for IL electrolytes. In conclusion, the IL based electrolytes containing **IL 8**, **13** and **16** exhibit a significantly better cycling performance than the conventional organic electrolyte. Therefore, the combination of the IL electrolytes and SIB electrodes can lead to superior charge-discharge properties in combination with high safety and stable performance of the SIB system, which is crucial for large-scale energy storage applications.[27] In order to further improve the systems and obtain more valuable information regarding the relation of the IL nature to the electrochemical performance, the remaining functionalized RTILs from Figure 2 have to be tested and evaluated as well. Moreover, detailed investigations based on XRD, XPS and EDX studies of the cycled NMO material have to be undertaken to explain the observed trends, enabling a tailored approach towards even better electrolytes.

Table 2: Data of the electrochemical coin cell studies. [a] Conducting salt: NaFSI (0.5 M). [b] EC/PC = 1/1 wt%; conducting salt: $NaClO_4$ (1.0 M). [c] Initial discharge capacity (2nd cycle). [d] Retention after 350 cycles.

Coin cell	Electrolyte	Cap_{In} [mAh/g][c]	R [%][d]	D_{Na^+} [cm^2/s]
CC_2	IL 2[a]	168.5	27	4.67×10^{-15}
CC_8	IL 8[a]	140.6	74	5.97×10^{-15}
CC_{13}	IL 13[a]	165.9	70	1.32×10^{-14}
CC_{16}	IL 16[a]	100.7	81	3.63×10^{-15}
CC_{Org}	EC/PC[b]	175.5	32	2.39×10^{-14}

Experimental

Characterization methods

Thermal stability: Thermogravimetric analysis (TGA) was carried out on a Q5000 by *TA Instruments*. Measurements were conducted under argon with a heating rate of 10 K/min and an offset temperature of 600 °C. The obtained mass loss in dependence of time was evaluated by the software TA Universal Analysis. T_d was defined as the temperature at the inflection point of the weight loss curve (that is the maximum of the 1st deviation), since this a reproducible and distinct method.
Viscosity: The dynamic viscosity was measured with microVISC viscosimeter from *RheoSense* with the measuring cell B-10 at 23 °C.
Conductivity: Electrochemical conductivities were determined at 23 °C in an argon-filled glovebox using a *Mettler Toledo* InLab 751 conductivity probe head connected to a *Solartron* SI1260 frequency response analyzer. The samples were placed in a small test tube inserted into a custom made, temperature-controlled steel block. A full impedance spectrum was recorded with an alternating current voltage of 0.02 V and in a frequency range between 1 Hz and 10 MHz. The ohmic resistance of the electrolyte was determined based on the real part of the impedance where the imaginary part of the impedance is (close to) 0. The specific conductivity was determined using a cell constant of 1 cm^{-1} calibrated with 0.1 M KCl. For the temperature dependent measurements, conductivities were reported in steps of 5 °C with a tolerance of ± 0.2 °C.
Linear sweep voltammetry: LSV curves were recorded under argon using a PGSTAT302N potentiostat from *Metrohm Autolab*. Measurements were conducted in a three electrode setup (sample volume: 0.2 ml, electrode distance: 3 mm) applying a glassy carbon working electrode, a Pt wire as counter electrode and an Ag/AgCl reference electrode. The respective cathodic and anodic stability limits were referenced to the Fc/Fc^+ redox couple and defined as the potentials at the cut-off current density of 1 mA/cm^2 in the first scan.[49]
Electrochemical measurements: Galvanostatic charge/discharge tests were carried out in the voltage range from 1.5 to 3.8 V vs. Na/Na^+ on a *Neware* battery tester system under ambient conditions. For the determination of the diffusion coefficient, cyclic voltammetry (CV) curves were recorded using a *BioLogic* VMP3 potentiostat (1.5 and 3.8 V vs. Na/Na^+).

Synthesis and characterization of the RTILs

Synthetic procedures and characterization of the RTILs is provided in the SI.

Electrochemical investigations

Coin cell preparation: The cathode material $Na_{0.6}Co_{0.1}Mn_{0.9}O_2$ was synthesized following a reported protocol.[13]
The IL electrolytes were prepared in an argon-filled glovebox by dissolving NaFSI (Nippon Shokubai) in the respective RTILs **2**, **8**, **13** and **16** to yield a concentration of 0.5 M. The solutions were continuously stirred for at least 24 h before use. For the organic electrolyte $NaClO_4$ (Sigma-Aldrich, ≥ 98%) was dissolved in a mixture of EC/PC (1:1 w/w, Sigma-Aldrich (EC: 99%; PC: ≥ 99.7%)) to yield a 1 M solution.
For preparation of the electrodes the active material was mixed with acetylene black (Alfa Aesar, > 99%) and polyvinylidene fluoride (PVdF, Arkema, Kynar HSV 900) with a weight ratio of 60:20:20 in N-methy1-2-pyrrolidone (NMP) (Sigma-Aldrich, 99%). The resulting cathode composite was coated on a battery grade aluminum foil (Goodfellow) using a doctor blade with a gap of 100 µm and subsequently dried at 80 °C to remove NMP. Electrodes with a diameter of 16 mm were obtained by punching. After drying at 110 °C under vacuum overnight the prepared electrodes were assembled in 2016 coin cells in an argon-filled glovebox (H_2O and O_2 < 0.1 ppm) with sodium metal (99.8%, Acros Organics) as anode and glass fiber (Grade GF/F - Whatman) as separator.
Galvanostatic cycling: Galvanostatic cycling tests were carried out in half cells employing NMO as the working electrode and metallic sodium as the counter/reference electrode. The cells were first charged to 3.8 V followed by discharging to 1.5 V at a rate of 50 mA/g.
Rate testing: The cells were cycled at different rates (20, 50, 100, 200, 400 mA/g) for 5 cycles each and cycled once again at 50 mA/g at the end of the test.
Diffusion coefficient: To determine the diffusion coefficients, the cells were subjected to cyclic voltammetry at different scan rates (0.1 mV/s, 0.2 mV/s, 0.5 mV/s, 1 mV/s and 2 mV/s). A plot of peak current versus the square root of scan rate is generated for both oxidation and reduction processes. From this plot, the slope was obtained and was used to calculate the diffusion coefficient from the Randles-Sevcik equation.[60]

Conclusion

In this contribution, different functionalized RTILs, based on Pyr, Pip, Mor and ammonium cationic core structures and TFSI and FSI anions are presented. The RTILs were obtained in high purity and with optimized low water content (< 5 ppm).
In a systematic study, the broad variety of synthesized RTILs was consistently analyzed under identical experimental conditions facilitating direct comparison of different RTILs. Focus was laid on the physicochemical properties of major importance for electrochemical applications: viscosity, conductivity, thermal and electrochemical stability. Evaluation and comparison of the data for the whole range of functionalized ILs revealed main trends. Viscosity and conductivity are mainly dependent on the functional group tethered to the cationic core structure as well as the anion of the respective ILs. The latter also has the highest impact on thermal stability. TFSI ILs exhibit significantly higher thermal stabilities compared to their FSI analogues. Besides the thioether functionalized IL **IL 4**, all investigated ILs show wide ESWs. Nature of the IL, i.e. functional group, cationic core and anion, mainly influences the distinct anodic and cathodic stability limits.
This systematic approach not only improves the basic understanding of the structural effect on the properties of ionic liquids, but also enriches the fundamental knowledge on ionic liquids, which is beneficial to design and optimize ionic liquids for several applications.
Based on the evaluated physicochemical properties, the ether functionalized TFSI ILs **IL 2**, **8**, **13** and **16** were chosen for more detailed electrochemical investigations in NMO half-cells. The results were compared with the performance of the conventionally applied organic electrolyte EC/PC ($NaClO_4$ 1 M). Coin cells with electrolytes containing **IL 8**, **13** and **16** showed enhanced cycling stability and significantly better capacity retention than the cells with the organic electrolyte implying a beneficial effect of the IL electrolytes on cell performance. Further, $\mathbf{CC_8}$, $\mathbf{CC_{13}}$ and $\mathbf{CC_{16}}$ were found to be stable to high rate cycling, indicating that these systems are reasonably stable to reversible sodiation at high rates and no considerable side reactions occur during the cycling.
These results clearly show that the IL electrolytes containing **IL 8**, **13** and **16** are compatible with the electrode materials and exhibit superior charge-discharge properties compared to the organic electrolyte. Combined with the enhanced safety due to the high thermal stability and non-flammability of the IL electrolytes such IL-SIBs fulfill essential requirements for large-scale energy storage systems.
More detailed studies of the electrode materials and the nature of the surface layers formed based on XRD, XPS and EDX will be undertaken in the future to reveal the reasons for the respective cycling stabilities. To examine the effect of other functional groups, e.g. nitrile, allyl or ester on the electrochemical cell performances and especially the SEI layer formation, coin cell tests with additional RTILs will be object of further studies. Based on the present extensive study, tailor made electrolyte mixtures can be designed to combine the optimized properties of the individual IL electrolytes and thus improve the overall electrochemical performance of IL-SIB systems.

Conflicts of interest

There are no conflicts to declare.

Acknowledgements

This work was supported by a PhD scholarship from the International Centre for Energy Research (ICER). The authors wish to acknowledge financial support from the National

Research Foundation of Singapore (NRF) investigator ship award (number NRF-NRFI2017-08) and the TUM Graduate School. L. Seidl, L. Asen, O. Schneider and T. Ludwig are acknowledged for support in the conductivity, TGA and viscosity measurements. Further, the authors thank J. Hornung for valuable discussions and proof reading.

References

1. C. Ding, T. Nohira, K. Kuroda, R. Hagiwara, A. Fukunaga, S. Sakai, K. Nitta and S. Inazawa, *J. Power Sources*, 2013, **238**, 296-300.
2. J. Liu, J.-G. Zhang, Z. Yang, J. P. Lemmon, C. Imhoff, G. L. Graff, L. Li, J. Hu, C. Wang, J. Xiao, G. Xia, V. V. Viswanathan, S. Baskaran, V. Sprenkle, X. Li, Y. Shao and B. Schwenzer, *Adv. Funct. Mater.*, 2013, **23**, 929-946.
3. M. Sawicki and L. L. Shaw, *RSC Adv.*, 2015, **5**, 53129-53154.
4. N. Wongittharom, C.-H. Wang, Y.-C. Wang, C.-H. Yang and J.-K. Chang, *ACS Appl. Mater. Interfaces*, 2014, **6**, 17564-17570.
5. K. Vignarooban, R. Kushagra, A. Elango, P. Badami, B. E. Mellander, X. Xu, T. G. Tucker, C. Nam and A. M. Kannan, *Int. J. Hydrogen Energy*, 2016, **41**, 2829-2846.
6. H. Pan, Y.-S. Hu and L. Chen, *Energ. Environ. Sci.*, 2013, **6**, 2338-2360.
7. C.-H. Wang, Y.-W. Yeh, N. Wongittharom, Y.-C. Wang, C.-J. Tseng, S.-W. Lee, W.-S. Chang and J.-K. Chang, *J. Power Sources*, 2015, **274**, 1016-1023.
8. J. Serra Moreno, G. Maresca, S. Panero, B. Scrosati and G. B. Appetecchi, *Electrochem. Commun.*, 2014, **43**, 1-4.
9. A. Ponrouch, D. Monti, A. Boschin, B. Steen, P. Johansson and M. R. Palacín, *J. Mater. Chem. A*, 2015, **3**, 22-42.
10. L. G. Chagas, D. Buchholz, L. Wu, B. Vortmann and S. Passerini, *J. Power Sources*, 2014, **247**, 377-383.
11. N. Wongittharom, T.-C. Lee, C.-H. Wang, Y.-C. Wang and J.-K. Chang, *J. Mater. Chem. A*, 2014, **2**, 5655-5661.
12. D. Su, C. Wang, H.-J. Ahn and G. Wang, *Chem. Eur. J.*, 2013, **19**, 10884-10889.
13. N. Bucher, S. Hartung, J. B. Franklin, A. M. Wise, L. Y. Lim, H.-Y. Chen, J. N. Weker, M. F. Toney and M. Srinivasan, *Chem. Mater.*, 2016, **28**, 2041-2051.
14. J. Kalhoff, G. G. Eshetu, D. Bresser and S. Passerini, *ChemSusChem*, 2015, **8**, 2154-2175.
15. J. I. Kim, K. Y. Chung and J. H. Park, *Journal of Membrane Science*, 2018, **566**, 122-128.
16. F. Colò, F. Bella, J. R. Nair and C. Gerbaldi, *J. Power Sources*, 2017, **365**, 293-302.
17. F. Bella, F. Colò, J. R. Nair and C. Gerbaldi, *ChemSusChem*, 2015, **8**, 3668-3676.
18. R. D. Rogers, *Science*, 2003, **302**, 792-793.
19. T. Welton, *Chem. Rev.*, 1999, **99**, 2071-2084.
20. J. P. Hallett and T. Welton, *Chem. Rev.*, 2011, **111**, 3508-3576.
21. D. D. Patel and J. M. Lee, *Chem. Rec.*, 2012, **12**, 329-355.
22. N. Bucher, S. Hartung, M. Arkhipova, D. Yu, P. Kratzer, G. Maas, M. Srinivasan and H. E. Hoster, *RSC Adv.*, 2014, **4**, 1996-2003.
23. D. Betz, P. Altmann, M. Cokoja, W. A. Herrmann and F. E. Kühn, *Coord. Chem. Rev.*, 2011, **255**, 1518-1540.
24. J. W. Kück, R. M. Reich and F. E. Kühn, *Chem. Rec.*, 2016, **16**, 349-364.
25. M. Cokoja, R. M. Reich, M. E. Wilhelm, M. Kaposi, J. Schäffer, D. S. Morris, C. J. Münchmeyer, M. H. Anthofer, I. I. E. Markovits, F. E. Kühn, W. A. Herrmann, A. Jess and J. B. Love, *ChemSusChem*, 2016, **9**, 1773-1776.
26. M. Galiński, A. Lewandowski and I. Stępniak, *Electrochim. Acta*, 2006, **51**, 5567-5580.
27. C.-H. Wang, C.-H. Yang and J.-K. Chang, *Chem. Commun.*, 2016, **52**, 10890-10893.
28. A. Lewandowski and A. Świderska-Mocek, *J. Power Sources*, 2009, **194**, 601-609.
29. Z. B. Zhou, H. Matsumoto and K. Tatsumi, *Chem. Eur. J.*, 2006, **12**, 2196-2212.
30. G. A. Elia, U. Ulissi, S. Jeong, S. Passerini and J. Hassoun, *Energ. Environ. Sci.*, 2016, **9**, 3210-3220.
31. T. Yim, M.-S. Kwon, J. Mun and K. T. Lee, *Isr. J. Chem.*, 2015, **55**, 586-598.
32. Z. Chen, Y. Huo, J. Cao, L. Xu and S. Zhang, *Ind. Eng. Chem. Res*, 2016, **55**, 11589-11596.
33. M. Egashira, H. Todo, N. Yoshimoto, M. Morita and J.-I. Yamaki, *J. Power Sources*, 2007, **174**, 560-564.
34. J.-T. Lee, Y.-W. Lin and Y.-S. Jan, *J. Power Sources*, 2004, **132**, 244-248.
35. M. Egashira, S. Okada, J.-i. Yamaki, D. A. Dri, F. Bonadies and B. Scrosati, *J. Power Sources*, 2004, **138**, 240-244.
36. X. Cao, X. He, J. Wang, H. D. Liu, S. Roser, B. R. Rad, M. Evertz, B. Streipert, J. Li, R. Wagner, M. Winter and I. Cekic-Laskovic, *ACS Appl. Mater. Interfaces*, 2016, **8**, 25971-25978.
37. X. Cao, S. Röser, B. Rezaeirad, X. He, B. Streipert, M. Winter and I. Cekic-Laskovic, *Z. Anorg. Allg. Chem.*, 2015, **641**, 2536-2542.
38. C. Maton, N. De Vos and C. V. Stevens, *Chem. Soc. Rev.*, 2013, **42**, 5963-5977.
39. M. H. Ibrahim, M. Hayyan, M. A. Hashim, A. Hayyan and M. K. Hadj-Kali, *Fluid Phase Equilib.*, 2016, **427**, 18-26.
40. G. B. Appetecchi, M. Montanino, M. Carewska, M. Moreno, F. Alessandrini and S. Passerini, *Electrochim. Acta*, 2011, **56**, 1300-1307.
41. H.-B. Han, K. Liu, S.-W. Feng, S.-S. Zhou, W.-F. Feng, J. Nie, H. Li, X.-J. Huang, H. Matsumoto, M. Armand and Z.-B. Zhou, *Electrochim. Acta*, 2010, **55**, 7134-7144.
42. O. O. Okoturo and T. J. VanderNoot, *J. Electroanal. Chem.*, 2004, **568**, 167-181.
43. C. M. Forsyth, D. R. MacFarlane, J. J. Golding, J. Huang, J. Sun and M. Forsyth, *Chem. Mater.*, 2002, **14**, 2103-2108.
44. P. Bonhôte, A.-P. Dias, N. Papageorgiou, K. Kalyanasundaram and M. Grätzel, *Inorg. Chem.*, 1996, **35**, 1168-1178.
45. J. Reiter, E. Paillard, L. Grande, M. Winter and S. Passerini, *Electrochim. Acta*, 2013, **91**, 101-107.
46. J. S. Lee, N. D. Quan, J. M. Hwang, J. Y. Bae, H. Kim, B. W. Cho, H. S. Kim and H. Lee, *Electrochem. Commun.*, 2006, **8**, 460-464.
47. H. Sakaebe and H. Matsumoto, *Electrochem. Commun.*, 2003, **5**, 594-598.
48. C. Ding, T. Nohira, R. Hagiwara, K. Matsumoto, Y. Okamoto, A. Fukunaga, S. Sakai, K. Nitta and S. Inazawa, *J. Power Sources*, 2014, **269**, 124-128.
49. Z. Xue, L. Qin, J. Jiang, T. Mu and G. Gao, *Phys. Chem. Chem. Phys.*, 2018, **20**, 8382-8402.
50. H.-B. Han, Y.-X. Zhou, K. Liu, J. Nie, X.-J. Huang, M. Armand and Z.-B. Zhou, *Chem. Lett.*, 2010, **39**, 472-474.

51. Z. B. Zhou, H. Matsumoto and K. Tatsumi, *Chem. Eur. J.*, 2005, **11**, 752-766.
52. A. Bhide, J. Hofmann, A. Katharina Dürr, J. Janek and P. Adelhelm, *Phys. Chem. Chem. Phys.*, 2014, **16**, 1987-1998.
53. A. A. J. Torriero, A. I. Siriwardana, A. M. Bond, I. M. Burgar, N. F. Dunlop, G. B. Deacon and D. R. MacFarlane, *J. Phys. Chem. B*, 2009, **113**, 11222-11231.
54. H. Matsumoto, H. Sakaebe and K. Tatsumi, *J. Power Sources*, 2005, **146**, 45-50.
55. G. B. Appetecchi, M. Montanino, D. Zane, M. Carewska, F. Alessandrini and S. Passerini, *Electrochim. Acta*, 2009, **54**, 1325-1332.
56. T. Yim, C. Y. Choi, J. Mun, S. M. Oh and Y. G. Kim, *Molecules*, 2009, **14**, 1840-1851.
57. R.-S. Kühnel, D. Reber and C. Battaglia, *ACS Energy Letters*, 2017, **2**, 2005-2006.
58. R. S. Kühnel, D. Reber, A. Remhof, R. Figi, D. Bleiner and C. Battaglia, *Chem. Commun.*, 2016, **52**, 10435-10438.
59. L. Suo, O. Borodin, T. Gao, M. Olguin, J. Ho, X. Fan, C. Luo, C. Wang and K. Xu, *Science*, 2015, **350**, 938-943.
60. N. Arun, V. Aravindan, W. C. Ling and S. Madhavi, *J. Power Sources*, 2015, **280**, 240-245.

Journal Name

ARTICLE

Graphical Abstract